ChemComm
Chemical Communications

Accepted Manuscript

This article can be cited before page numbers have been issued, to do this please use: G. Durin, M. Lee, M. A. Pogany, C. Kahl, T. Weyhermueller, W. Leitner and N. Kaeffer, *Chem. Commun.*, 2024, DOI: 10.1039/D4CC04050C.

ROYAL SOCIETY OF CHEMISTRY

rsc.li/chemcomm

ChemComm

View Article Online
DOI: 10.1039/D4CC04050C

COMMUNICATION

Electrochemical Aldehydes Hydrogenation: Probing the Inner-Sphere Strategy with Nickel-Bipyridine Complexes†

Received 00th January 20xx,
Accepted 00th January 20xx

DOI: 10.1039/x0xx00000x

Gabriel Durin,‡[a,b] Mijung Lee,‡[a] Martina A. Pogany,‡[a] Christian Kahl,[a] Thomas Weyhermüller,[a] Walter Leitner,[a,c] Nicolas Kaeffer[a]*

Developing electrohydrogenation routes for organics is crucial in synthesis electrification. Here, we interrogate the electrocatalytic hydrogenation of aldehydes through an inner-sphere mechanism at a nickel-bipyridine complex. An (electro)reduction triggers the coordination of the aldehyde into a key nickeloxirane species, which affords hydrogenation products by stroichiometric protonations. Turnover yet remains challenging with acids suitable for electrocatalytic conditions due to sluggish proton transfers, which we probe by combined reactivity and computational studies.

The electrification of synthetic processes is empowering renewable and sustainable resources in chemistry.[1-5] That virtuous approach is often propelled by electrocatalysis to warrant energy efficiency and selectivity. Key to the rational development of these electrocatalytic systems is to decode the mechanisms involved. Molecular complexes are particularly handy in that context, as their well-defined nature facilitates access to mechanistic information. This strategy has namely led to molecular electrocatalytic systems for the hydrogenation of organic multiple bonds.[6-17] Surprisingly, and in contrast to CO_2 reduction, electrocatalytic hydrogenation (ECH) of organic carbonyls with molecular complexes remains scarcely explored.[18] Siewert and co-workers demonstrated the repurpose of {Mn(bpy)}-type hydrogenation electrocatalysts from CO_2 to organic carbonyls, including aliphatic aldehydes,[15, 16] while Waymouth and co-workers addressed the challenging ECH of benzaldehyde using a Mo Shvo-type complex[14] (Scheme 1). These systems perform hydrogenation through the evolution of a metal hydride that is transferred to the electrophilic C–O carbon. In our exploration of electrocatalyzed synthesis, we have recently employed the coordination ability of nickel-bipyridine complexes to achieve alkyne ECH through successive electron and proton transfers, bypassing metal hydride intermediates.[19, 20] This approach exploits hydride-free, selective pathways that are at odds with catalysis in thermal hydrogenation and reported ECHs. Here, we investigate the challenges in transposing the hydride-free strategy from the hydrogenation of C–C multiple bonds towards that of C–O ones (Scheme 1).

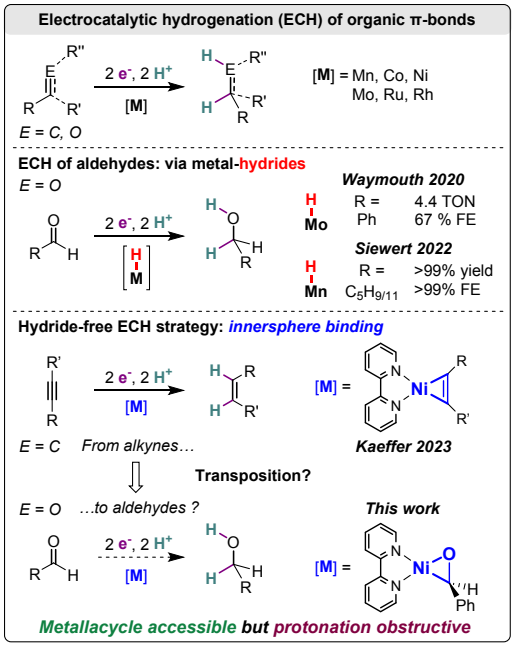

Scheme 1. Electrocatalytic hydrogenation of C–O and C–C multiple bonds by molecular complexes including nickel-bipyridine complexes.

Knowing that [Ni(bpy)(BzO)$_2$] (**1**) is a hydrogenation electrocatalyst for alkyne substrates, we aimed at probing this complex for carbonyl ones.

[a]*Max Planck Institute for Chemical Energy Conversion, Stiftstrasse 34-36, 45470 Mülheim an der Ruhr, Germany*
[b]*Université Grenoble Alpes, DCM, CNRS, 38000 Grenoble, France*
[c]*Institut für Technische und Makromolekulare Chemie, RWTH Aachen University, Worringerweg 2, 52074 Aachen, Germany*
**Email: nicolas.kaeffer@cec.mpg.de*
† Electronic Supplementary Information (ESI) available. See DOI: 10.1039/x0xx00000x
‡ These authors contributed equally to this work.

ChemComm

View Article Online
DOI: 10.1039/D4CC04050C

COMMUNICATION

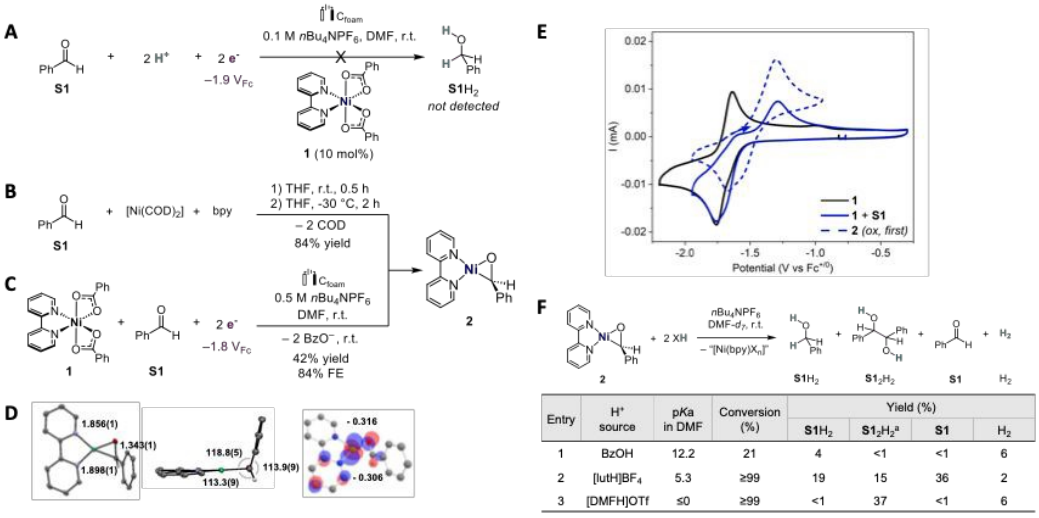

Entry	H+ source	pKa in DMF	Conversion (%)	Yield (%)			
				S1H2	S1H2a	S1	H2
1	BzOH	12.2	21	4	<1	<1	6
2	[lutH]BF4	5.3	≥99	19	15	36	2
3	[DMFH]OTf	≤0	≥99	<1	37	<1	6

Scheme 2. A. Electrocatalytic attempt using **1** (1 mM), **S1** (10 mM) and BzOH (22 mM) after passing 8.5 C (ca 2e⁻/**S1**). **B.** Synthesis of **2** from [Ni(COD)$_2$]. **C.** Electrosynthesis of **2** from **1** at E_{app} = –1.80 V_{Fc} (charge = 4.56 C; ca 1e⁻/**1**). **D.** Molecular structure of **2** obtained by XRD (ORTEP; 50% probability; color code: gray: C; purple: N; green: Ni; red: O; white: H) and computed electron density of the HOMO of **2** with Mulliken charges at aldehydic C and O (H atoms omitted for clarity, except aldehydic ones). **E.** CVs of **1**, **1** and **S1**, and **2** (1 mM each; 0.1 V·s^{-1} scan rate). **F.** Protonation reactions starting from **2** (at 30 min). Unless otherwise stated, the supporting electrolyte is DMF 0.1 M nBu$_4$NPF$_6$.[a]Maximum theoretical yield 50%.

However, electrolysis of benzaldehyde (**S1**) in the presence of **1** and benzoic acid (BzOH) as proton source leads to marginal conversion and no detected hydrogenation product **S1**H$_2$, once passed ca 2 electrons per **S1** (Scheme 2A). Varying the solvent (e.g. DMSO, THF) or even the substrate (*p*-MeO-PhCHO) was not productive. Moreover, more cathodic applied potentials (see ESI Section 3.4) or more acidic conditions (e.g. [DMFH]OTf) trigger the direct reduction of **S1** at the electrode[21] and are hence not compatible with this system.

The absence of catalysis thus questions whether a pathway involving a nickelacyclic intermediate, in analogy to the nickelacyclopropene reported for alkyne semihydrogenation, is viable in the case of C=O bond hydrogenation. To interrogate the formation of such species in the case of C–O unsaturations, a 1:1 mixture of [Ni(COD)$_2$] (COD = 1,4- cyclooctadiene) and 2,2'-bipyridine was reacted with benzaldehyde (**S1**) in THF, inspired by literature and our precedents.[20, 22, 23] The reaction quickly evolves a green precipitate identified after work-up as the nickeloxirane [Ni(bpy)(PhCHO)][22-24] (**2**) obtained in 84% yield (Scheme 2B; ESI section 2.1). The molecular structure elucidated by single crystal X-ray diffraction (XRD) evidences a planar geometry for the nickeloxirane **2** (Scheme 2D; ESI section 2.4), with a C–O bond length of 1.343 Å, quite elongated relative to **S1** (1.210 Å).[25] Moreover, the ^{1}H NMR signature (DMSO-d_6) attributed to the aldehydic hydrogen of **2** manifests by a broad singlet at 5.05 ppm, in a region typical of benzylic resonances (vs. 10.02 ppm in free **S1**), and the C–O stretching frequency at 1360 cm^{-1} in **2** undergoes a substantial red-shift compared to free **S1** (ν(C=O) = 1693 cm^{-1}). This spectroscopic evidence further reinforces the C–O single-bond character in **2** (see ESI Section 2).

Investigating now the voltammetric behavior of **1** shows that the addition of aldehyde **S1** (1 equiv.) triggers the reduction wave at $E_{p,c}$ = –1.76 V_{Fc}[20] to evolve a shoulder (E ≈ –1.70 V_{Fc}) and lose reversibility (Scheme 2E). Most importantly, these changes are accompanied by the build-up of an anodic wave at $E_{p,a}$ = – 1.29 V_{Fc} matching that observed for the oxidation of native **2**. These points suggest that **2** can also be formed by reductive electrogeneration from **1** and **S1**. Bulk reductive electrolysis of a mixture of **1** and **S1** at E_{app} = –1.80 V_{Fc} (**1**/**S1** 1:1 ratio, ca 1e⁻/**1**) (Scheme 2C) further confirms the electrogeneration of **2** in 42% yield and 84% faradaic efficiency as revealed by the characteristic voltammetric and ^{1}H NMR signatures (ESI section 4.4).

While these results demonstrate binding and activation of **S1** in the nickelacyclic species **2**, including under electroreductive conditions, protonation is required to release the hydrogenated product and induce turnover. Addition of 2 equivalents of BzOH (p*K*a 12.2 in DMF[26]) to **2** dissolved in DMF-d_7, nBu$_4$NPF$_6$ 20 mM (r.t.) affords after 30 min 21% conversion of **2** and a 4% yield in **S1**H$_2$ with H$_2$ as byproduct (6% yield) (Scheme 2F; Entry 1). Extending reaction time to 24 h leads to full conversion and **S1**H$_2$ in 17% yield (see ESI section 4.1 for additional details). These results indicate a slow reactivity of BzOH with **2**, leading both to hydrogenation into **S1**H$_2$ and hydrogen evolution (HER). The latter reactivity suggests the formation of nickel hydride species, while the former can also proceed by protonations of the metallacycle as observed with alkynes.[20]

To interrogate if stronger acids would accelerate the reaction or promote one reaction pattern over the other, we tested 2,6-lutidinium (lutH$^+$ p*K*a 5.3 in DMF;[27, 28] Scheme 2F; Entry 2). After 30 min, **2** is fully converted and affords **S1**H_2 in 19% yield and low hydrogen evolution (2%). Two additional points are yet worth a note. First, the pinacol coupling product hydrobenzoin (**S1**$_2H_2$) is detected in substantial yields (15%). Second, significant amounts of unreacted **S1** are released (36%), which indicate the displacement of that substrate from the Ni center. We surmise that this expulsion is induced by the coordination of the proton source at Ni, potentially leading to a hydride species as [Ni(bpy)(lut)(H)]$^+$. That hypothesis is reinforced by the observation of a ^{1}H NMR signal at –21.74 ppm (Figure S14) attributed to such Ni–H hydride compounds by comparison with literature data.[29, 30] The concomitant observation of the Ni-H species and free **S1** supports that this hydride is not highly reactive towards the aldehyde. In the case of the more acidic DMFH$^+$ (p*K*a ≤ 0 in DMF[26, 28]), the selectivity in **S1**-derived products is now fully switched to **S1**$_2H_2$ (Scheme 2F; Entry 3), while a Ni–H is also detected (Figure S14). The increased selectivity towards the product **S1**$_2H_2$ when Ni–H are detected suggests a 1e$^-$/1H$^+$-reactivity[31] of these hydrides.

We further explored conditions for hydrogenation (see ESI sections 4.1-4.3). With **2**, the use of alternative Brønsted acids does not improve yields in hydrogenated products and Lewis acids do not afford hydrogenation. Regarding ligands, the more electron-poor 4,4-bis(trifluoromethyl)-2,2'-bipyridine fails to generate an aldehyde adduct, but a nickeloxirane forms using the electron-donating 4,4-bis(methoxy)-2,2'-bipyridine, which in turn leads to similar protonation results. In general, the combination of **2** and lutH$^+$ provides the highest yield in **S1**H_2.

Taken together, these results indicate that (electro)reductive generation of **S1** into the nickelacyclic species **2** is feasible, but subsequent reactivity is undermined by competing hydride formation or slow protonations at **S1**. While lutH$^+$ or DMFH$^+$ afford fast conversion of **2** into hydrogenation products of **S1**, these proton sources are too acidic for the investigated electrocatalytic potentials. At contrast, the less acidic BzOH appropriate to ECH of alkyne leads here to a sluggish reactivity. To further uncover the mechanistic limitations and the underpinning distinctions from the operating alkyne ECH case, we employed DFT calculations (Scheme 3). We considered an initiation from **1** by 2-electron reduction associated with the release of a benzoate ligand leading to **I1** as previously described[20] and used as the reference entry point. The binding of **S1** to **I1** by associative displacement of BzO$^-$ is both kinetically facile (**TS$_{S1\text{-}I1}$** at +2.8 kcal·mol^{-1}) and highly favored, leading to the nickeloxirane **2** as the most stable computed intermediate (ΔG = –23.8 kcal·mol^{-1}). We note that, aside from being a relevant species by electrochemical access, **2** is also the starting material in our stoichiometric experiments. We then investigated protonation at the substrate sites in **2**, namely at the C or the O atom in the nickelacycle. The calculated O-protonation has a reachable transition state (**TS$_{2\text{-}I2}$** at ΔΔG‡= +14.7 kcal·mol^{-1}), but the formation of the nickel-alkyl species **I2** is endergonic (ΔΔG= +5.4 kcal·mol^{-1}). Furthermore, this intermediate appears unproductive since neither protonation nor isomerization seem plausible (see ESI section 5.2). On the other hand, C-protonation is computed to afford a relatively stable benzolate complex **I3** (ΔG = –21.3 kcal·mol^{-1}), from which a second O-protonation is feasible to release the desired product **S1**H_2. However, the initial C-protonation is hindered by a high energy cost at **TS$_{2\text{-}I3}$** (ΔΔG‡= +26.1 kcal·mol^{-1}). Interestingly, β-H elimination, which would have contributed to the hydride pathway (HER), from **I2** and **I3** are unlikely, with TSs >27 kcal·mol^{-1}. Consequently, computational results support that protonations of **2** by BzOH are difficult and, within computational uncertainty, close to feasibility limits at RT (> 23 kcal·mol^{-1}), further corroborating the slow and understoichiometric evolution of **S1**H_2 observed in chemical conditions.

We next turned to the formation of hydride species to trace back HER with our system. The electrogeneration of **I1** from the precatalyst **1** can lead to slow HER via the hydride complex **IH**, as previously described.[20] However, **I1** is not relevant in stoichiometric experiments with **2**, yet producing H_2. In that case, we found that the oxidative addition of BzOH at **2** leads barrierless to the hydride **I4**, thus bringing back the occurrence of HER. The span of that pathway is relatively high (+25.8 kcal·mol^{-1}) but cannot be fully discarded within the uncertainty of the calculations, hence is a possible account for H_2 produced.

For the formation of the hydrobenzoin **S1**$_2H_2$, a radical pathway resulting from the homolytic cleavage of the Ni–C bond of **I2** (BDFE = 34.6 kcal·mol^{-1}) seems reasonable. Another pathway involving ring-expansion by addition of **S1** to **2** proved too high in energy (> 29 kcal·mol^{-1}; see ESI section 5.2).

Interestingly, **S1** binding into **2** and **IH** hydride generation are both expected fast from **I1**, with respective computed TSs of 2.8 and 6.2 kcal·mol^{-1}, but **2** is strongly stabilized versus **IH** by 7.7 kcal·mol^{-1}.

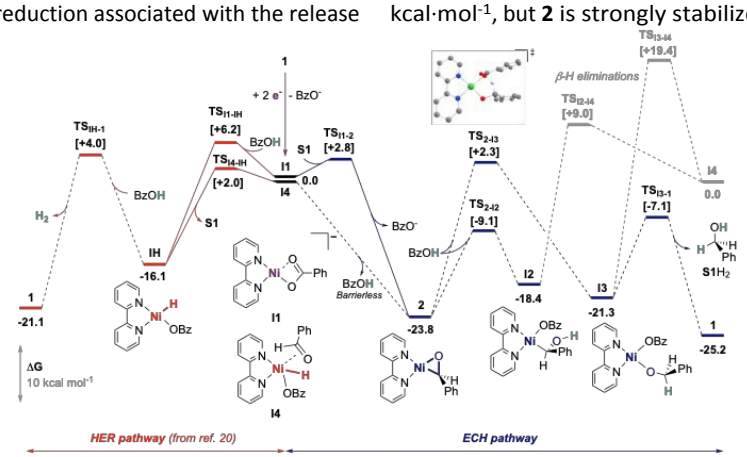

Scheme 3. Computed HER (red)[20] and ECH (blue) pathways at PBE-D3/6-311+G(d,p) level of theory using CPCM model to account for solvent effect (DMF).

ChemComm

View Article Online
DOI: 10.1039/D4CC04050C

COMMUNICATION

The accumulation of the nickelaoxirane is therefore plausible in the hypothesis of slow subsequent kinetics supported by the elevated spans. Along this line, in the voltammetry of **1** recorded with excess BzOH, the addition of 1 equivalent of **S1** restores the electrochemical signature of **2** (Figure S9). This displacement of the electrochemical systems towards **2** even in the presence of BzOH corroborates the thermodynamic preference of the nickelaoxirane versus the hydride species and further shows that **S1** inhibits HER. We note that this relative stability with respect to **IH** is lower for nickeloxirane as compared to nickelacyclopropene (ΔG(metallacycle→IH) = 7.7 *vs* 13.9 kcal·mol^{-1}), supporting a more accessible nickel-hydride in the case of aldehyde as substrate.

In summary, in an approach to transpose a hydride-free electrocatalytic hydrogenation from C–C to C–O π-bonds, we demonstrated the successful (electro)generation of a key nickeloxirane species, leading to hydrogenation products by stoichiometric protonation. Identifying efficient electrocatalytic conditions yet remains challenging. We diagnosed that inner-sphere substrate binding is here again preferred over hydride formation, but subsequent protonations of the nickelacyclic species are obstructive. These findings will guide uncovering further molecular catalysis for carbonyl electrohydrogenation.

Data availability

The data supporting this article are included as part of the Supplementary Information. Crystallographic data for **2** has been deposited at the CCDC under number 2374778.

Conflicts of interest

There are no conflicts to declare.

Notes and references

1. A. Wiebe, T. Gieshoff, S. Mohle, E. Rodrigo, M. Zirbes and S. R. Waldvogel, *Angew. Chem. Int. Ed.*, 2018, **57**, 5594-5619.
2. N. Kaeffer and W. Leitner, *JACS Au*, 2022, **2**, 1266-1289.
3. N. von Wolff, O. Rivada-Wheelaghan and D. Tocqueville, *ChemElectroChem*, 2021, **8**, 4019-4027.
4. G. Centi, S. Perathoner, C. Genovese and R. Arrigo, *Chem. Commun.*, 2023, **59**, 3005-3023.
5. Z. Liu, L. Zhang, Z. Ren and J. Zhang, *Chem. Eur. J.*, 2023, **29**, e202202979.
6. J. Derosa, P. Garrido-Barros and J. C. Peters, *J. Am. Chem. Soc.*, 2021, **143**, 9303-9307.
7. J. Derosa, P. Garrido-Barros, M. Li and J. C. Peters, *J. Am. Chem. Soc.*, 2022, **144**, 20118-20125.
8. S. Gnaim, A. Bauer, H.-J. Zhang, L. Chen, C. Gannett, C. A. Malapit, D. E. Hill, D. Vogt, T. Tang, R. A. Daley, W. Hao, R. Zeng, M. Quertenmont, W. D. Beck, E. Kandahari, J. C. Vantourout, P.-G. Echeverria, H. D. Abruna, D. G. Blackmond, S. D. Minteer, S. E. Reisman, M. S. Sigman and P. S. Baran, *Nature*, 2022, **605**, 687-695.
9. X. Wu, C. N. Gannett, J. Liu, R. Zeng, L. F. T. Novaes, H. Wang, H. D. Abruña and S. Lin, *J. Am. Chem. Soc.*, 2022, **144**, 17783-17791.
10. I. M. F. De Oliveira and J.-C. Moutet, *J. Mol. Catal.*, 1993, **81**, L19-L24.
11. J.-C. Moutet, L. Yao Cho, C. Duboc-Toia, S. Ménage, E. C. Riesgo and R. P. Thummel, *New J. Chem.*, 1999, **23**, 939-944.
12. H. Shimakoshi, Z. Luo, K. Tomita and Y. Hisaeda, *J. Organomet. Chem.*, 2017, **839**, 71-77.
13. M. H. Rønne, D. Cho, M. R. Madsen, J. B. Jakobsen, S. Eom, É. Escoudé, H. C. D. Hammershøj, D. U. Nielsen, S. U. Pedersen, M.-H. Baik, T. Skrydstrup and K. Daasbjerg, *J. Am. Chem. Soc.*, 2020, **142**, 4265-4275.
14. K. C. Armstrong and R. M. Waymouth, *Organometallics*, 2020, **39**, 4415-4419.
15. I. Fokin and I. Siewert, *Chem. Eur. J.*, 2020, **26**, 14137-14143.
16. I. Fokin, K.-T. Kuessner and I. Siewert, *ACS Catal.*, 2022, **12**, 8632-8640.
17. D. P. Marron, C. M. Galvin, J. M. Dressel and R. M. Waymouth, *J. Am. Chem. Soc.*, 2024, **146**, 17075-17083.
18. G. Durin, N. Kaeffer and W. Leitner, *Curr. Opin. Electrochem.*, 2023, **41**, 101371.
19. M. Y. Lee, C. Kahl, N. Kaeffer and W. Leitner, *JACS Au*, 2022, **2**, 573-578.
20. G. Durin, M. Y. Lee, M. A. Pogany, T. Weyhermuller, N. Kaeffer and W. Leitner, *J. Am. Chem. Soc.*, 2023, **145**, 17103-17111.
21. M. Chandrasekaran, M. Noel and V. Krishnan, *J. Electroanal. Chem.*, 1991, **303**, 185-197.
22. E. Dinjus, I. Gorski, H. Matschiner, E. Uhlig and D. Walther, *Z. Anorg. Allg. Chem.*, 1977, **436**, 39-46.
23. E. Dinjus, H. Langbein and D. Walther, *J. Organomet. Chem.*, 1978, **152**, 229-237.
24. We note that the synthesis of **2** had been previously reported in ref. 23, but with partial characterization (elemental analysis, infrared and ultraviolet-visible spectroscopies).
25. K. B. Borisenko, C. W. Bock and I. Hargittai, *J. Phys. Chem.*, 1996, **100**, 7426-7434.
26. V. Fourmond, P. A. Jacques, M. Fontecave and V. Artero, *Inorg. Chem.*, 2010, **49**, 10338-10347.
27. A. Kütt, S. Tshepelevitsh, J. Saame, M. Lõkov, I. Kaljurand, S. Selberg and I. Leito, *Eur. J. Org. Chem.*, 2021, **2021**, 1407-1419.
28. L. Sooväli, I. Kaljurand, A. Kütt and I. Leito, *Analytica Chimica Acta*, 2006, **566**, 290-303.
29. J. Breitenfeld, O. Vechorkin, C. Corminboeuf, R. Scopelliti and X. Hu, *Organometallics*, 2010, **29**, 3686-3689.
30. A. K. Ravn, M. B. Johansen and T. Skrydstrup, *Angew. Chem. Int. Ed.*, 2022, **61**, e202112390.
31. M. J. Chalkley, P. Garrido-Barros and J. C. Peters, *Science*, 2020, **369**, 850-854.

View Article Online
DOI: 10.1039/D4CC04050C

Data Availability Statement

Electrochemical Aldehydes Hydrogenation: Probing the Inner-Sphere Strategy with Nickel-Bipyridine Complexes

Gabriel Durin,[‡a,b] Mijung Lee,[‡a] Martina A. Pogany,[‡a] Christian Kahl,[a] Thomas Weyhermüller,[a] Walter Leitner,[a,c] Nicolas Kaeffer[a]*

[a]*Max Planck Institute for Chemical Energy Conversion, Stiftstrasse 34-36, 45470 Mülheim an der Ruhr, Germany*
[b]*Université Grenoble Alpes, DCM, CNRS, 38000 Grenoble, France*
[c]*Institut für Technische und Makromolekulare Chemie, RWTH Aachen University, Worringerweg 2, 52074 Aachen, Germany*

*Corresponding author: Nicolas Kaeffer (nicolas.kaeffer@cec.mpg.de)

The data supporting this article have been included as part of the Supplementary Information.
Crystallographic data for **2** has been deposited at the CCDC under number 2374778.